JMEPEG (2012) 21:770–776
DOI: 10.1007/s11665-012-0129-z

1059-9495/$19.00

Characterization of Dissimilar Linear Friction Welds of α-β Titanium Alloys

Yina Guo, Yulung Chiu, Moataz M. Attallah, Hangyue Li, Simon Bray, and Paul Bowen

(Submitted October 29, 2011; in revised form December 9, 2011)

Characterization of dissimilar linear friction weld (LFW) of Ti-alloys has been carried out. The microstructure of a Ti-64 with Ti-6246 weld was analyzed using scanning and transmission electron microscopy. The microtexture of the weld was examined using electron back-scattered diffraction (EBSD) and the microhardness was measured. The dissimilar LFW weld shows an interface at the central weld zone (CWZ) with strong contrast. The element distribution measured using energy-dispersive X-ray spectrometer suggests that only limited atomic diffusion occurred during welding. In the weld region, the hardness of Ti-64 shows an increase while that of Ti-6246 shows a decrease, compared with the respective parent materials in as-welded condition. After post-weld heat treatment, a hardness increase was observed in Ti-6246, while Ti-64 shows no significant hardness increase. Although the EBSD pattern quality is poor in the CWZ at the as-welded condition, the pattern quality of the post-weld heat-treated sample shows that both the Ti-64 and Ti-6246 have similar texture.

Keywords dissimilar weld, EBSD, linear friction welding, SEM, TEM, Ti-64, Ti-6246

1. Introduction

Linear friction welding (LFW) is a solid-state joining process, suitable for joining non-axisymmetric work pieces. The two parts are joined by the heat generated between them due to the work of friction forces under pressure. Because of the relatively high capital investment required, LFW has been used mainly for the joining of high value-added components where the significant machine and associated tooling costs can be justified (Ref 1). To date, the main application of LFW is in the aerospace industry for joining titanium components, such as blades and discs (Ref 2).

A considerable amount of work has been carried out to gain a better understanding of the welding process, the resultant microstructure and mechanical properties of the joints (Ref 3-10). It has been found that LFWed titanium alloys often have higher strength in the weld region compared to base metal (Ref 6, 9). LFW joints can be characterized by several regions containing different microstructures. No widely accepted terminology exists for the weld regions. In the present study, four zones are used to describe the weld microstructure and are defined as follows:

- The central weld zone (CWZ), where the microstructure has been completely changed but no trace of the plastic deformation occurred in the welding can be identified.
- The thermo-mechanically affected zone (TMAZ), where elongation of microstructural features can be observed.
- The heat-affected zone (HAZ), where no visible plastic deformation exists but microstructure changes can be identified.
- The parent materials where the microstructure has not been affected.

LFW is able to join two different materials. However, research about the LFW of these dissimilar materials is very limited (Ref 11-13). LFW of dissimilar materials faces potential issues, as joining materials with different thermal expansion coefficients may lead to higher thermal stresses and ensuing cracking in the CWZ (Ref 14). Juhas et al. (Ref 12) and Baeslack et al. (Ref 13) studied titanium aluminides-titanium alloy dissimilar welds and found that the high peak temperature and the appreciable deformation experienced during LFW promoted the dynamic recrystallization of β grains, and the β decomposition to fine martensitic microstructures results in very high hardness in the weld region. Corzo et al. (Ref 11) studied the hardness of LFWed Ti-64-Ti-6242 and Ti-6246-Ti-6242 welds using indentation experiments. However, there has been no detailed microstructure characterization of dissimilar LFWs. As such, as part of a systematic microstructure study of LFWs, this paper summarizes results on the microhardness and microstructure characterization of a Ti-64-Ti-6246 dissimilar weld, at both as-welded and post-weld heat-treated (PWHTed) conditions.

This article is an invited submission to JMEP selected from presentations at the Symposia "Wetting, soldering and brazing" and "Diffusion bonding and characterization" belonging to the Topic "Joining" at the European Congress and Exhibition on Advanced Materials and Processes (EUROMAT 2011), held September 12-15, 2011, in Montpellier, France, and has been expanded from the original presentation.

Yina Guo, Yulung Chiu, Moataz M. Attallah, Hangyue Li, and **Paul Bowen**, School of Metallurgy and Materials, University of Birmingham, Birmingham B15 2TT, UK; and **Simon Bray**, Rolls-Royce plc, PO Box 31, Derby DE24 8BJ, UK. Contact e-mails: guoyina2001@gmail.com, y.chiu@bham.ac.uk, AttallMM@bham.ac.uk, H.Y.Li.1@bham.ac.uk, simon.bray@rolls-royce.com, and bowenp@adf.bham.ac.uk.

2. Materials and Experimental Procedure

The typical microstructures of the parent materials, Ti-6Al-4V (Ti-64) and Ti-6Al-2Sn-4Zr-6Mo (Ti-6246), are shown in Fig. 1 and the chemical compositions measured from the different phases in Tables 1 and 2. The Ti-6246 parent material has basket-weave microstructure with relatively thick primary α and β phases (secondary α can been seen embedded in the β phase as shown in the insertion). The Ti-64 has a fully equiaxed structure. PWHT was carried out at 600 °C for 1 h and followed by air cooling.

Microstructure characterization was carried out on a JOEL 7000 field-emission gunned scanning electron microscope (SEM) equipped with an Oxford INCA EDX software and an electron back-scattered diffraction (EBSD) system, and a JEM 2100 and a Tecnai F20 transmission electron microscope (TEM). For TEM investigation, 200 kV accelerating voltage was used. A Mitutoyo MVK-H1 hardness tester was used to obtain the hardness profile across the weld interface with a 300 μm separation, under 500 gf load and 10 s loading time.

3. Results and Discussion

3.1 Microhardness Profile

The microhardness profiles obtained from the as-welded and the PWHTed welds are shown in Fig. 2. The Ti-6246 parent material has an average hardness value of about 420 Hv, noticeably higher than that of the Ti-64 parent material of about 350 Hv. For the as-welded specimen, it is clear that the hardness of the Ti-6246 weld is generally of about 50 Hv lower than that of the parent material. Although a small peak can be seen at about 0.6 mm from the weld interface, overall the hardness is lower within a region of about 1.8 mm from the weld interface. On the Ti-64 side, the hardness increases from the parent material towards the weld interface and shows a rapid increase from the position at about 1.2 mm from the weld interface to about 400 Hv at the vicinity of the interface. After PWHT, the hardness of Ti-6246 shows a dramatic increase in the weld region and the highest hardness value of about 520 Hv appears in the CWZ, while the hardness value for Ti-64 does not show much change. The hardness of the parent materials shows a slight decrease upon the PWHT.

Table 1 Chemical compositions (wt.%) of the different phases in Ti-64 base metal measured using EDS

	Ti (wt.%)	Al (wt.%)	V (wt.%)	Fe (wt.%)
Primary α	90.5	7.2	2.3	…
Intergranular β	79.3	4.1	15.2	1.4

Table 2 Chemical compositions (wt.%) of the different phases in Ti-6246 base metal measured using EDS

	Ti (wt.%)	Al (wt.%)	Sn (wt.%)	Zr (wt.%)	Mo (wt.%)
Primary α	84.0	6.7	2.1	3.9	3.3
Retained β	79.6	5.1	2.2	4.9	8.2
Secondary α	82.0	5.3	2.2	3.9	6.6

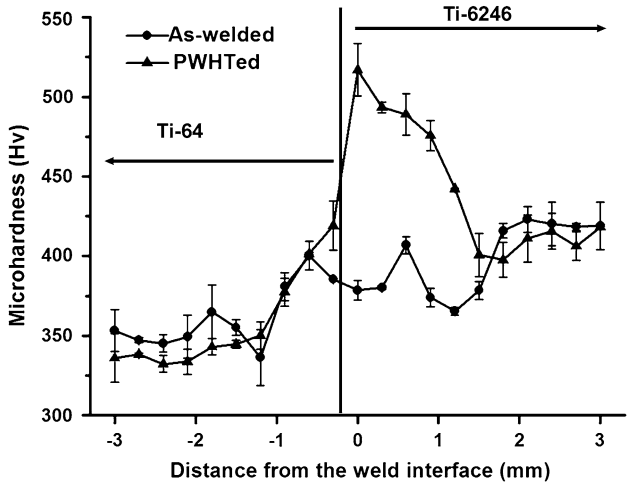

Fig. 2 Microhardness profiles measured perpendicular to the weld interface at the edge of as-welded (circles) and PWHTed (triangles) samples showing the hardness distribution across the weld interface

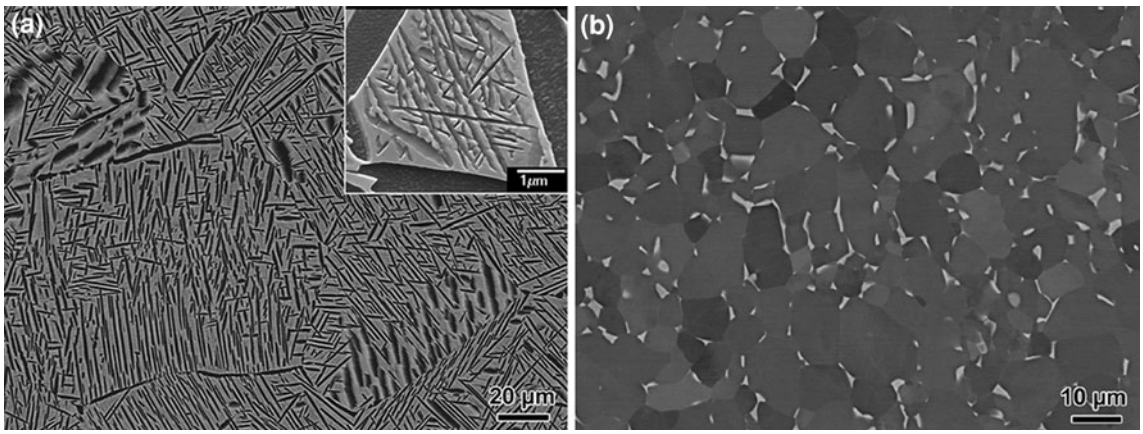

Fig. 1 Backscattered electron images showing the microstructures of base materials. (a) Ti-6246, primary α and retained β with fine secondary α inside (inserted image is a secondary electron image showing secondary α imbedded in β). (b) Ti-64, equiaxed α grains and intergranular β

3.2 Microstructure

Figure 3(a) shows a low magnification overview of a weld imaged using the back-scattered electrons. The weld interface which appears wavy can be clearly identified due to the strong contrast between the two alloys. On both sides, the microstructure shows a gradual change from the weld interface towards the parent materials. The different regions (positions A-F in Fig. 3a) in the weld were studied using SEM at higher magnification and shown in Fig. 3(b). On both the Ti-64 and Ti-6246, the microstructures are similar to those reported (Ref 15, 16).

In the HAZ of Ti-6246 side (marked as A in Fig. 3b), the image of secondary α becomes less clear and the quantity decreased comparing with that in the parent material, indicating that the temperature in this region during welding may have caused the dissolution of some of the secondary α. In contrast, the primary α remained unchanged. The most obvious microstructure change in TMAZ (marked as B in Fig. 3b) is the

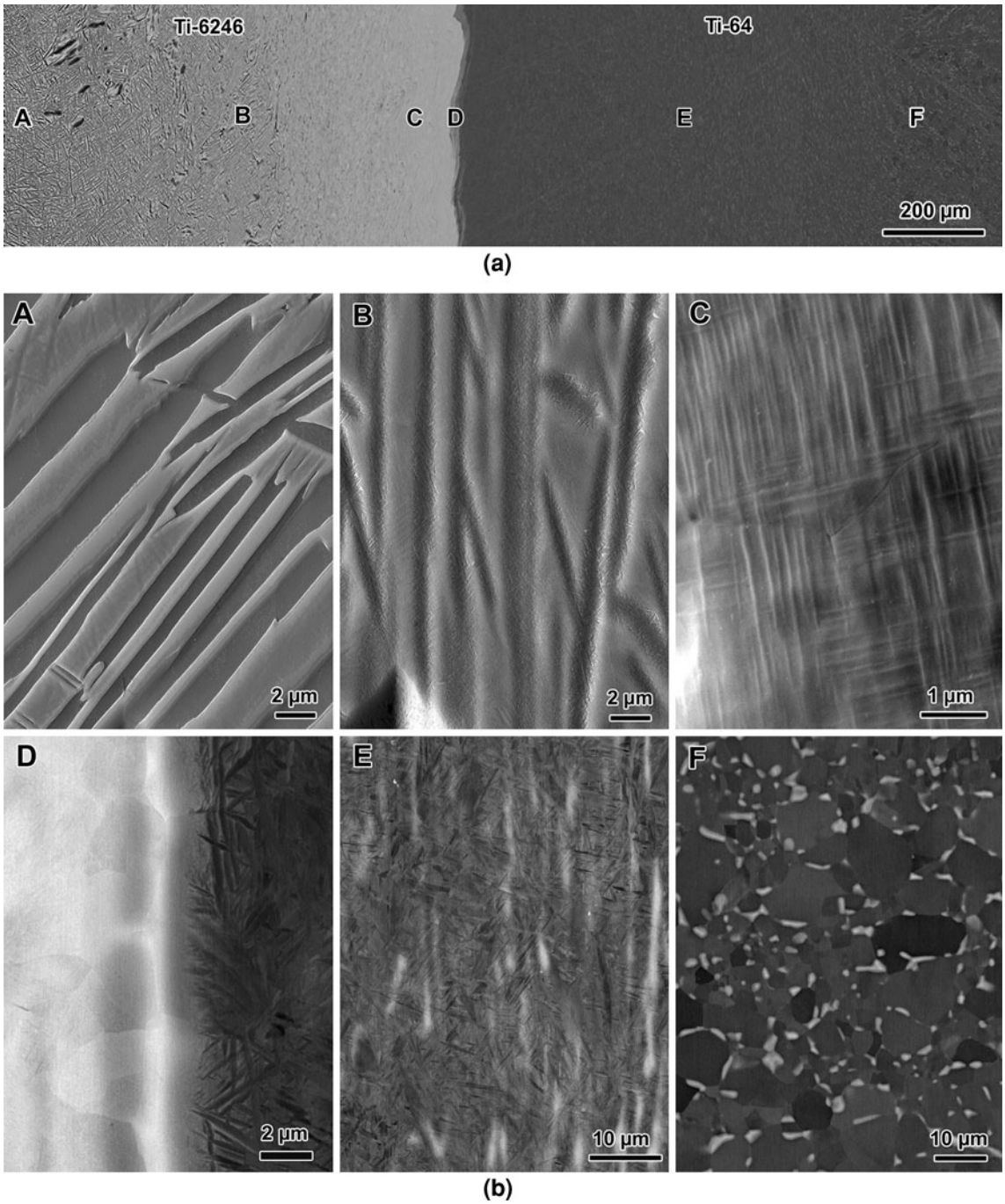

Fig. 3 SEM images showing the microstructure development across the weld interface. (a) Backscattered electron image montage showing the overview of the microstructure variation across the weld interface. The letters A to F represent the areas in the different weld zones. (b) SEM images showing microstructures of the relevant areas marked in (a), A, B, and C show the HAZ, TMAZ, and CWZ in Ti-6246 side, respectively. D shows the weld interface, E and F represent the TMAZ and HAZ in Ti-64 side

elongation of the primary α and the retained β along the oscillation direction, which indicates the severe plastic deformation during welding. Fine α can be seen along the interface of β and primary α. The CWZ microstructure (marked as C in Fig. 3b) was characterized by two sets of fine acicular-shaped features perpendicular to each other. In the HAZ of Ti-64 side (marked as F in Fig. 3b), the boundaries between α and β becomes less clearly defined comparing with those in the parent material. In the TMAZ (marked as E in Fig. 3b), grains are elongated and re-orientated along the oscillation direction. In TMAZ the remaining β (brighter phase) are elongated severely. The CWZ has a completely different microstructure compared to parent material, showing fine acicular microstructural features. At the center of the weld (marked as D in Fig. 3b), although different contrast can be clearly observed between the two alloys, no distinct interface can be identified. In the Ti-6246 side, grains of 2-5 μm can be clearly seen. However, the grain boundaries are not clear in the Ti-64 side.

3.3 Characterization of the CWZ

The microstructure of the CWZ was further studied. In the as-welded condition, as shown in Fig. 4(a), the microstructure of the Ti-64 consists of narrow laths of HCP crystal structure, as evidenced by the [1 $\bar{2}$10] diffraction pattern shown in Fig. 4(b). In the Ti-6246 side, careful tilting experiment shows the existence of very fine reticulate precipitates (see Fig. 4c). However, the diffraction pattern (as shown in Fig. 4d) is dominated by the reflections from the BCC β with very weak streaks presumably caused by the fine precipitates. It is likely that the fine precipitates are highly coherent with the β matrix and the reflections from these precipitates are too weak to be recorded using the digital camera used in this study. Further characterization of these fine precipitates will be needed.

Figure 5(a) shows a backscattered electron SEM image of the weld interface together with the positions for the energy-dispersive X-ray spectrometer (EDX) measurements carried out in SEM. The corresponding composition profile is shown in Fig. 5(b). As can be seen, the distribution of alloying elements is asymmetrical, showing their nominal concentration. No long-range inter-diffusion across the interface can be observed, in accordance with literature on Ti-14Al-21Nb and Ti-6242 study (Ref 12). This may be caused by the fact that during the welding the total period of time where the temperature is above the β-transus temperature is very short, thus leading to only limited atomic diffusion.

The microstructure of the PWHTed weld can be seen in Fig. 6. In Ti-64, hexagonal structure can be clearly identified (as exemplified by the [0 $\bar{1}$11] diffraction pattern Fig. 6a), though the microstructural features has been coarsened comparing with those at as-welded condition. In Ti-6246 side, no β grain can be identified while fine α variants exist. The

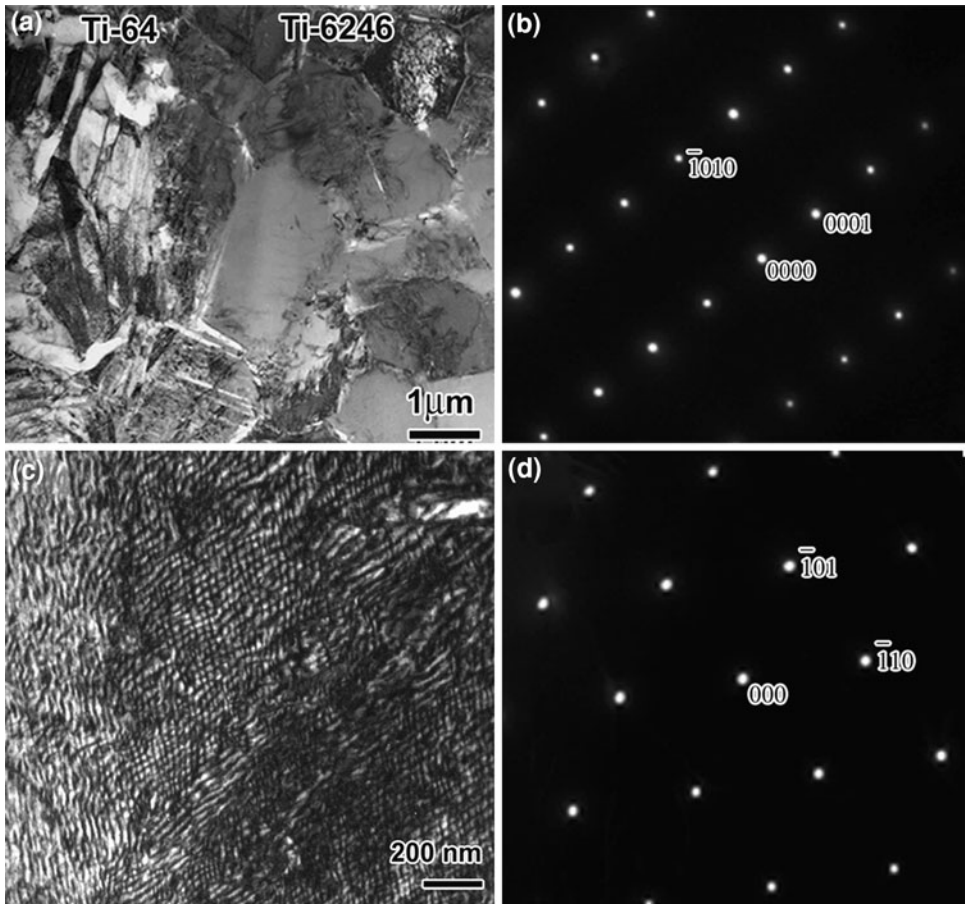

Fig. 4 TEM results showing the weld interface in the as-welded sample. (a) Bright field image of weld interface. (b) Selected area diffraction pattern taken from Ti-64 side showing [1 $\bar{2}$10] zone diffraction pattern in HCP structure. (c) Bright field image showing the netlike precipitation in β phase. (d) Diffraction pattern obtained in β grain in Ti-6246 side, no obvious reflection can be seen except the [111] BCC reflections

diffraction pattern (Fig. 6c) shows the overlapped reflections from two variants, one long [1 $\bar{2}$10] zone and the other along [1 $\bar{2}$13] zone of the HCP structure. The hardness change observed in the Ti-6246 side may be caused by the β → α″ → α phase transformations which have been observed in the quenched and aged Ti-6246 alloy (see Ref 17 for details).

EBSD was carried out to investigate microtexture development in the CWZ in both as-welded and PWHTed conditions. The pattern recognition rates were fairly low due to the fine microstructure and the residual stresses in this area caused by the fast cooling rate experienced in the welding process. Pattern recognition rate of about 65% was achieved in the PWHTed sample and the results acquired in this condition are depicted in Fig. 7. Figure 7(a) shows the SEM image of the CWZ and Fig. 7(b) the α phase orientation image mapping of the same area. The pole figures obtained were shown in Fig. 7(c)-(e) for α and β phases. The pole figures were generated separately for Ti-6246 and Ti-64 using the same reference coordinates, shown at the bottom right of the figure. The intensity of the texture expressed as the times of random texture is placed next to each pair of pole figures. The black pixels in Fig. 7(b) represent either β phase or un-recognized pixels. Figure 7(b)-(d) shows that the LFW has a very pronounced texture in both α and β phases within the CWZ of Ti-6246. The orientation map and the $\{0001\}_\alpha$ and $\{11\ \bar{2}0\}_\alpha$ pole figures obtained in Ti-64 shown in Fig. 7(e) are in conformity with those previously reported for the LFW Ti-64 welds (Ref 7, 15). The α phase tends to align with its *c*-axis lying in the weld interface plane and perpendicular to the oscillation direction. Due to the limited amount of β phase in Ti-64, the pole figures of β phase are not displayed here.

Although the total measured area is not particularly large, Fig. 7(d) shows that the β phase in the PWHTed Ti-6246 has a strong texture. This implies that similarly strong texture exist in the as-welded condition as it is known that the currently used heat-treatment parameters will not alter the crystallography texture of the alloys (Ref 7). In other words, although its origin remains to be clarified, it can be deduced that the CWZ of the as-welded Ti-6246 has strong β texture.

Since no α phase has been clearly identified in the as-welded sample (see Fig. 4), suggesting that the α phase was formed during the PWHT. Combining Fig. 7(c) and (d), it clearly shows that only one α variant was populated, resulting in a

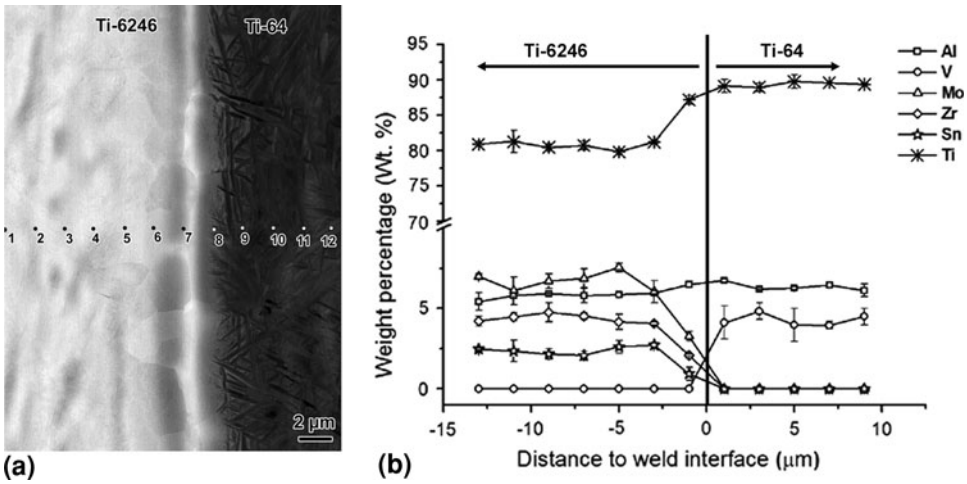

Fig. 5 SEM/EDX measurement shows the distribution of the alloying elements across the weld interface in as-welded sample. (a) Backscattered electron image showing the trace of EDX measurements, where point 1 is about 13 μm from the interface. (b) Relevant chemical composition profiles measured by EDX

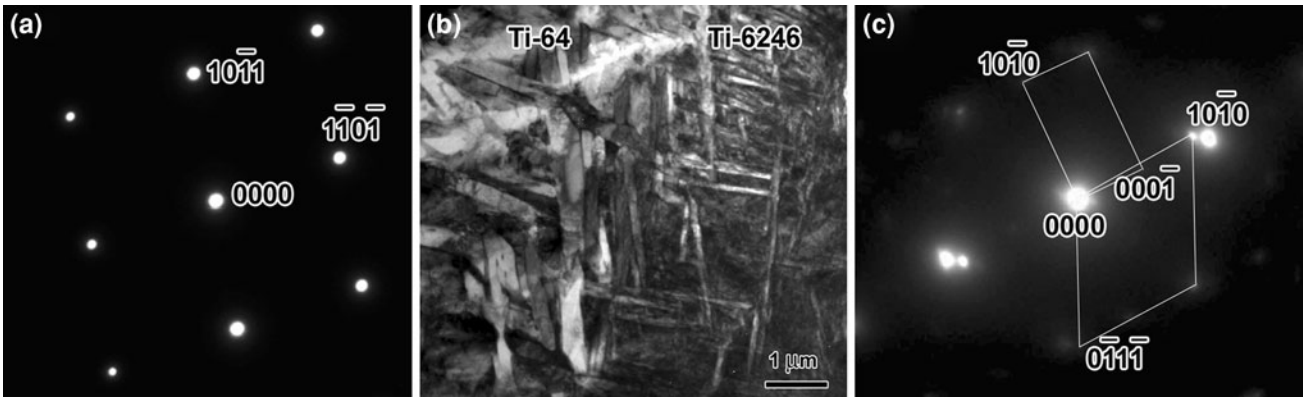

Fig. 6 TEM results showing the weld interface in the PWHTed sample. (a) Selected area diffraction pattern taken from Ti-64 side showing [0 $\bar{1}$11] zone diffraction pattern in HCP structure. (b) Bright field image of weld interface. (c) Diffraction pattern obtained in prior β grain in Ti-6246 side showing the overlapping of [1 $\bar{2}$10] and [1 $\bar{2}$13] zone reflections, indicating HCP structure

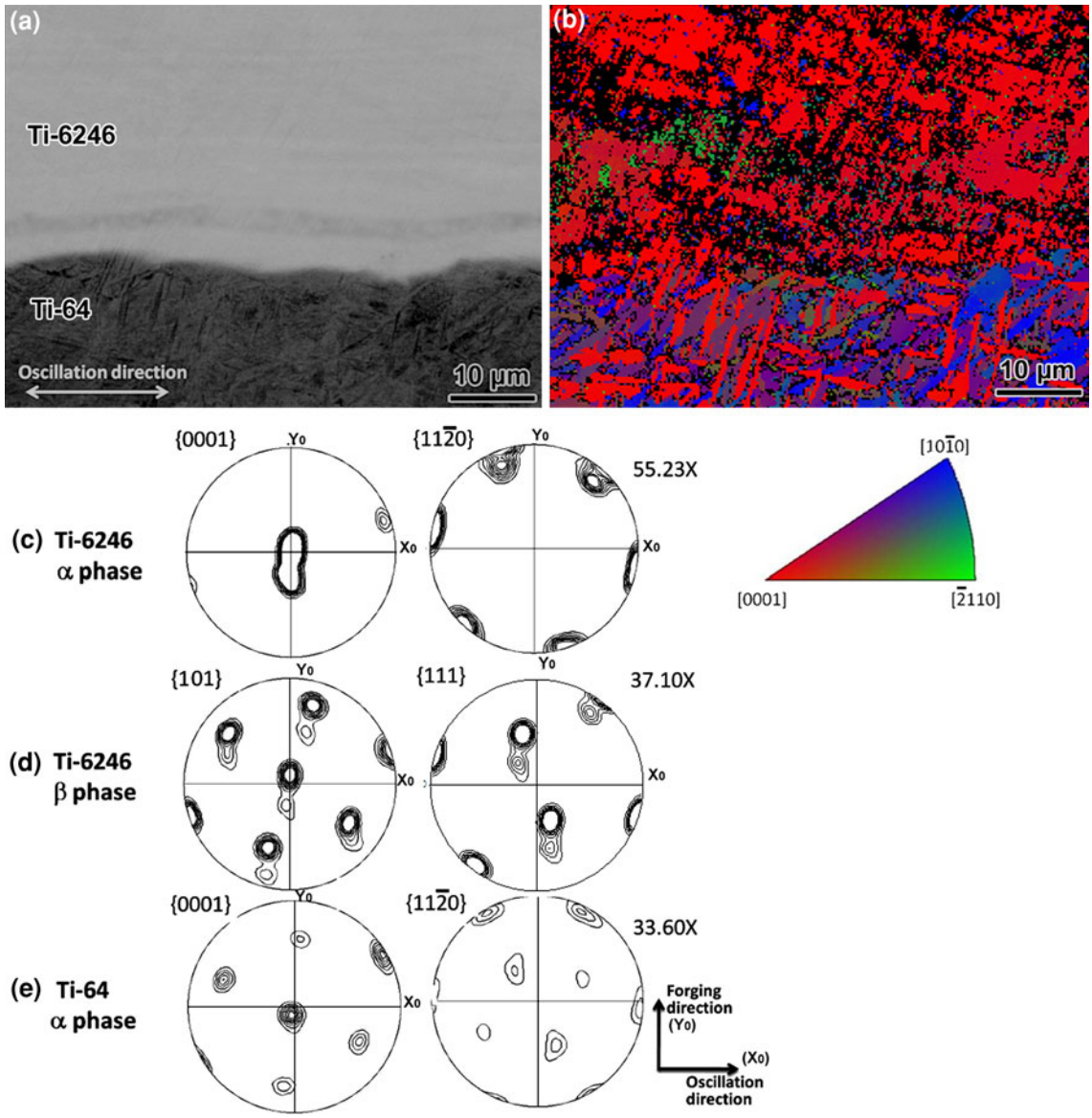

Fig. 7 EBSD mapping illustrating the texture development in the CWZ of the PWHTed sample. (a) Backscattered electron image showing the microstructure of the area measured by EBSD. (b) α Orientation map together with color key showing crystal alignment in the normal direction of the sample. (c, d) α and β pole figures for Ti-6246. (e) α Pole figures for Ti-64. For all the pole figures, Y_0-axis is parallel to forge pressure direction and X_0-axis is parallel to oscillation direction

strong texture with {0001} pole parallel to the sample normal. Although many researchers have demonstrated that the final α phase texture maybe affected by the α phase variant selection when cooling down from the β regime during thermo-mechanical processing of titanium alloys (see for example Ref 18). To the authors' best knowledge, such a preferred texture evolution of α phase from a heavily textured β during heat-treatment at intermediate temperature (such as the 600 °C used in the present study) has not been reported. However, fine precipitates coherent with the β matrix have been observed in the as-welded condition (Fig. 4d). Although the nature of these fine precipitates remains to be identified, it is possible that they may act as the precursor to the α nucleation/growth thus result in the α texture formation during the PWHT. Further work on the precipitate characterization and its relationship with the α phase formation during the PWHT will be necessary for a fuller understanding of the texture evolution.

4. Conclusions

The microstructure of a dissimilar Ti-6246 and Ti-64 weld has been characterized. The most surprising observations from this current study include:

(1) At the CWZ in Ti-6246 side, the β grain has been populated with very fine precipitates apparently highly coherent with the matrix. The nature of the fine precipitates remains to be clarified.
(2) The heavy texture of β and α in the PWHTed CWZ of Ti-6246. This suggests a similarly strong texture exist of the as-welded sample which could not be successfully measured due to probably the residual stress associated.
(3) The fine precipitates in the CWZ of the as-welded Ti-6246 may serve as precursor to the α nucleation/growth,

which eventually leads to a strong α texture upon the PWHT.

Acknowledgments

This work has been financially supported by an EPSRC—Rolls-Royce Strategic Partnership programme (EP/H500367/1). YG is grateful to the UK government for a Dorothy Hodgkin scholarship and Dr. Martin Strangwood for helpful discussion. Mr. Taenam Jung is gratefully thanked for his assistance in performing some of the experiments included in this paper.

References

1. B. Crossland, Friction Welding, *Contemp. Phys.*, 1971, **12**(6), p 559–574
2. I. Bhamji, M. Preuss, and P. Threadgill, Solid State Joining of Metals by Linear Friction Welding, *Mater. Sci. Technol.*, 2011, **27**(1), p 1–12
3. A. Vairis and M. Frost, High Frequency Linear Friction Welding of a Titanium Alloy, *Wear*, 1998, **217**(1), p 117–131
4. A. Vairis and M. Frost, On the Extrusion Stage of Linear Friction Welding of Ti 6Al 4V, *Mater. Sci. Eng. A*, 1999, **271**(1–2), p 477–484
5. M. Preuss, J. Quinta da Fonseca, A. Steuwer, L. Wang, P.J. Withers, and S. Bray, Residual Stresses in Linear Friction Welded IMI550, *J. Neutron Res.*, 2004, **12**(1–3), p 165–173
6. P. Wanjara and M. Jahazi, Linear Friction Welding of Ti-6Al-4V: Processing, Microstructure, and Mechanical-Property Inter-Relationships, *Metall. Mater. Trans. A*, 2005, **36A**, p 2149–2164
7. M. Karadge, M.P.C. Lovell, P.J. Withers, and S. Bray, Texture Development in Ti-6Al-4V Linear Friction Welds, *Mater. Sci. Eng. A*, 2007, **459**, p 182–191
8. J. Romero, M.M. Attallah, M. Preuss, M. Karadge, and S. Bray, Effect of the Forging Pressure on the Microstructure and Residual Stress Development in Ti-6Al-4V Linear Friction Welds, *Acta Mater.*, 2009, **57**(18), p 5582–5592
9. W.Y. Li, T.J. Ma, Y. Zhang, Q.Z. Xu, J.L. Li, S.Q. Yang, and H.L. Liao, Microstructure Characterization and Mechanical Properties of Linear Friction Welded Ti-6Al-4V Alloy, *Adv. Eng. Mater.*, 2008, **10**(1–2), p 89–92
10. R. Turner, J.-C. Gebelin, R.M. Ward, and R.C. Reed, Linear Friction Welding of Ti-6Al-4V: Modelling and Validation, *Acta Mater.*, 2011, **59**(10), p 3792–3803
11. V. Corzo, O. Casals, J. Alcala, A. Meteo, and M. Anglada, Mechanical Evolution of Linear Friction Welds in Titanium Alloys Through Indentation Experiments, *Weld. Int.*, 2007, **21**(2), p 125–129
12. M.C. Juhas, W.A. Baeslack III, H.L. Fraser, P. Threadgill, D. Phillips, and T.F. Broderick, Interface Characteristics of Solid-Phase Welds Between Ti-6Al-2Sn-4Zr-2Mo-0.1Si and Ti-14Al-21Nb Titanium Aluminide, *Titanium '92: Science and Technology, Proceedings of the Symposium, 7th World Titanium Conference*, 1992, San Diego, CA, United States, p 453–461
13. W.A. Baeslack III, T.F. Broderick, M. Juhas, and H.L. Fraser, Characterization of Solid-Phase Welds Between Ti-6Al-2Sn-4Zr-2Mo-0.1Si and Ti-13.5Al-21.5Nb Titanium Aluminide, *Mater. Charact.*, 1994, **33**, p 357–368
14. M. E. Nunn, Aero Engine Improvements Through Linear Friction Welding, *1st International Conference on Innovation and Integration in Aerospace Sciences*, 4-5 Aug 2005, Queen's University Belfast, Northern Ireland, UK, p 9
15. Y. Guo, Y.L. Chiu, H.Y. Li, M.M. Attallah, S. Bray, and P. Bowen, Microstructure and Microtexture of Linear Friction Welded Ti-6Al-4V, *The 12th World Conference on Titanium*, 19-22 June, Beijing, China, 2011 (in press)
16. M.M. Attallah, M. Preuss, and S. Bray, Microstructural Development During Linear Friction Welding of Titanium Alloys, *Trends in Welding Research 2008*, ASM International, 2009, p 486–491
17. M. Young, E. le Vine, and D. Margolin, Age Hardening of α- β Ti-6AI-2Sn-4Zr-6Mo, *Metall. Mater. Trans. A*, 1979, **10**(3), p 359–365
18. N. Gey, M. Humbert, M.J. Philippe, and R.Y. Combres, Modeling the Transformation Texture of Ti-64 Sheets After Rolling in the β-Field, *Mater. Sci. Eng.*, 1997, **230**(1–2), p 68–74